



# New Oral Coaxial Nanofibers for Gadodiamide-Prospective Intestinal Magnetic Resonance Imaging and Theranostic

This article was published in the following Dove Press journal:  
*International Journal of Nanomedicine*

Alaa Yaser Darwesh  
Marwa Salah El-Dahhan   
Mahasen Mohamed Meshali 

Department of Pharmaceutics, Faculty of Pharmacy, Mansoura University, Mansoura 35516, Egypt

**Purpose:** Gadodiamide (GDD) is a widely used magnetic resonance imaging (MRI) contrast agent. It is available only as intravenous injection. Unfortunately, it exhibits a high renal toxicity. In this respect, the author investigated the possibility of developing nanofibers (NFs, one-dimensional (1D) nanostructures) of GDD that would be promising for oral administration in intestinal imaging. NFs are prepared by electrospinning technique in which a strong electrostatic field is applied on a polymer solution.

**Methods:** NFs were prepared by coaxial electrospinning technique using Eudragit S100 (ES 100) as a shell layer and GDD loaded with polyvinylpyrrolidone K90 (PVP K90) and hydroxypropyl-beta-cyclodextrin (HP- $\beta$ -CyD) as core fibers. Compatibility study of the NFs ingredients was attested through ATR and DSC investigations. Thermogravimetric analysis of NFs was done to insure its stability. In vitro release of GDD in the intestinal medium with different pH values was measured. In vitro cytotoxicity test was done to prove its safety. Additionally, stability of NFs to perform its function was examined by X-ray.

**Results:** NFs experienced high entrapment efficiency of about  $94.3\% \pm 3.1\%$ . The ingredients of NFs were compatible through FT-IR and DSC study. The in vitro release data of GDD from coaxial NFs were slow ( $<14\%$ ) in pH 1.2 till 2 h, while at pH 7.4 it showed burst release of about 12% in the first 2 min. Thermogravimetric analysis proved the NFs are stable. The in vitro cytotoxicity study proved the safety of NFs. Using mammography, the coaxial NFs behaved the same as GDD plain indicating its ability to be a contrasting agent.

**Conclusion:** Coaxial NFs of GDD as a core with PVP K90 and HP- $\beta$ -CyD and ES 100 as a shell were stable and efficient as oral imaging dosage form for the intestine. It might be a prospective theranostic.

**Keywords:** gadodiamide, magnetic resonance imaging, coaxial nanofibers, contrast agent

## Introduction

Nanoparticulate delivery systems have been investigated widely in the pharmaceutical industry owing to protection from degradation in gastrointestinal tract (GIT), the ability to control release of drugs, improve the bioavailability, decreases the drug toxicity and increase patient's compliance with less frequent dosing.<sup>1,2</sup> Recently, nanofibers (NFs) have been evaluated for their ability to serve as novel controlled released system in pharmaceutical field.<sup>3</sup> This might be attributed to the fact that NFs size, surface area and porosity can be accurately controlled by varying different parameters. Electrospinning technology has guided huge attention over time. The mechanism depends on the utilization of a strong electrostatic field on a polymer solution to form ultrafine fibers.<sup>4</sup>

Correspondence: Alaa Yaser Darwesh  
Department of Pharmaceutics, Faculty of Pharmacy, Mansoura University,  
Mansoura, Egypt  
Tel +20 1063450461  
Fax +20 502247496  
Email alyaser\_2011@mans.edu.eg

Coaxial electrospinning was developed by applying certain modification of the conventional electrospinning process.<sup>5</sup> It is a simple technique which exploits electrical energy to prepare 1D nanoscale polymer fibers.<sup>5</sup> The process is also called co-electrospinning means the formulation of core-shell NFs which can be applied into several fields including biotechnology and drug delivery.<sup>6</sup> The technique is the same as conventional electrospinning except using coaxial needle instead of standard needle as spinneret.<sup>7</sup> The shell or sheath solution is attached to the outer needle and the core solution is connected to the inner needle. By controlling the flow rates of the two different solutions, a core shell droplet is formed at the tip of the coaxial needle which has a shape similar to the Taylor cone as a result of the pulling action of the electric Maxwell.<sup>8</sup>

Magnetic resonance imaging (MRI) is one of the most powerful noninvasive imaging techniques that offers visualization of anatomical structures with both high spatial resolution and unlimited tissue penetration depth.<sup>9</sup> MRI enables early diagnosis of many diseases including cancer, cardiovascular dysfunction, and problems related to the brain and central nervous system.<sup>10</sup> Despite the numerous advantages of this technique, the sensitivity of MRI images still needs to be improved. Developing MRI contrast agents with high efficiency and sensitivity will highlight the difference between normal and abnormal tissues.<sup>11</sup> MRI contrast agents rely on the modification of the longitudinal (T1) and transverse (T2) relaxation rates of the water protons, which give rise to positive and negative contrast, respectively.<sup>12</sup> Positive contrast is far more popular in the clinical community since it is easier to visualize bright areas on gray MRI images. To date, all commercial T1 contrast agents have been based on gadolinium-containing chelates.<sup>13</sup>

Gadolinium (Gd) was favored as the active center for first-generation commercial contrast complexes, given multiple favorable physiochemical properties. These properties include; seven unpaired electrons (distributed isotropically in its 4f shell), which offer an electrically charged magnetic center that exhibits the strongest effect of all the known elements on the length of T1 relaxation time.<sup>14</sup>

All transition metals exhibit intolerant toxicity.<sup>15</sup>  $Gd^{+3}$  metal forms acid solutions in water and insoluble hydroxides in solutions of neutral pH, which accumulate rapidly within the reticuloendothelial system (RES) following intravenous (IV) administration via phagocytosis by the

Kupffer cells in the liver.<sup>15</sup> Free gadolinium ( $Gd^{+3}$ ) is a very toxic heavy metal because its ionic radius is very similar to that of calcium. Free gadolinium can replace calcium in bone and block calcium channels. So, it can inhibit nerve transmissions, muscle contraction, blood coagulation, and mitochondrial function.<sup>16,17</sup> In order to mitigate toxicity, manufactured chelates are formed via a chelating process, in which an electronegative atom (chelating agent) donates an electron to the positively charged ion ( $Gd^{+3}$ ). The resultant large organic molecules form a more stable compound surrounding the Gd ion.<sup>18</sup> The Gd-based chelated agents (GBCAs) including Gadodiamide (GDD) have many advantages as a highly stable in neutral aqueous solution. These characteristics are general prerequisite for diagnostic agents (contrast agents) administered intravenously in small volumes.<sup>19</sup>

The only dosage form available for MRI diagnosis by GDD is intravenous solution. For gastrointestinal diagnosis, the chelated GDD is given with syrup orally which lack patient compliance.<sup>20</sup> The present study is aimed to prepare new solid dosage form of GDD as coaxial NFs to release GDD in the lower part of the GIT. This coaxial NFs will solve the nephrotoxicity problem accompanied with its use intravenously in the detection of gastrointestinal tract cancer.<sup>21</sup>

The aim of the current study was to design an optimized coaxial NFs of GDD. Polyvinylpyrrolidone K90 (PVP K90) and hydroxypropyl- $\beta$ -cyclodextrin (HP- $\beta$ -CyD) are the main polymers used to prepare the core of the GDD coaxial NFs. The shell of the coaxial NFs was made of Eudragit S 100 (ES 100) which is characterized by its high solubility at pH>7.4 to produce small and large intestine targeted NFs. The optimized formula was further subjected to in vitro release, as well as ingredient compatibility study and kinetic analysis of the release data. In vitro cytotoxicity and thermogravimetric analysis would be fulfilled. Finally, in vitro evaluation using X-ray was assessed.

## Materials and Methods

### Materials

Omniscan (Gadodiamide GDD, the gadolinium complex of diethylenetriamine pentaacetic acid bismethylamide) (287 mg/mL), produced by General Electric (G.E.). Polyvinylpyrrolidone (PVP K90) was purchased from Sigma-Aldrich Chemie GmbH, Germany (CAS: 9003-39-8, 99%). Hydroxypropyl-beta-cyclodextrin (HP- $\beta$ -CyD) was

purchased from XI'AN Health Biochem Technology Co., Ltd, China (CAS: 128446–35-5, 99.5%). Sodium saccharin was supplied by El Nasr Pharmaceutical and chemical Co., Cairo, Egypt (CAS: 6155–57-3, 99%). Eudragit S100 (ES 100) was procured from Evonik Röhm Pharma GmbH, Darmstadt, Germany (CAS: 25086–15-1). Absolute ethanol (CAS: 64–17-5, 99.8%) and glycerol (56–81-5, 99.5%) were obtained from Fischer Scientific UK.

## Preparation of GDD Loaded Coaxial NFs

GDD was available for MRI diagnosis as intravenous solution. For GIT diagnosis, it is given with syrup orally which lack patient compliance. In our study, preparation of coaxial NFs GDD was investigated to release GDD in the lower part of the GIT. Table 1 illustrates the difference between GDD (Omniscan) and coaxial NFs GDD. GDD-loaded coaxial NFs were prepared to encapsulate GDD in the core with PVP and HP- $\beta$ -CyD, then the fibers were surrounded with ES 100 sheath (Table 2).

## Preparation of Sheath NFs Solution

ES 100 (1.3 gm) was dissolved in 10 mL absolute ethanol using magnetic stirring (Heidolph, USA) for 30 min, Table 2. The produced viscous solution (sheath solution) was

**Table 1** The Difference Between GDD (Omniscan) and Coaxial NFs GDD

	GDD	GDD Coaxial NFs
Dosage form	clear, colorless to slightly yellow aqueous solution	Solid nanofibers (transparent)
Materials	Gadodiamide (287 mg/mL) + Sodium hydroxide (1M) or hydrochloric acid (1 M) + Water for injections.	Shell: ES-100 Core: GDD + PVP K90 + HP- $\beta$ -CyD + Sodium saccharin + Glycerol
Route of administration	Intravenous	Oral
Effect	Systematic for general MRI of the body after intravenous administration	Local effect inside the intestinal lumen
Side effect	Common side effects: nausea, dizziness, headache, pain at injection site, rash, itching, or hives.	Limited side effects proved by in vitro cytotoxicity

**Table 2** Compositions of the Solutions Used for Coaxial Electrospinning

Sheath Solution	Core Solution Composition
1.3 gm ES 100 Dissolved in 10 mL absolute ethanol	3 mL GDD 0.8 gm PVP K90 1.85 gm HP- $\beta$ -CyD 100 mg Sodium saccharine 0.2 mL Glycerol 7 mL absolute ethanol

**Notes:**GDD gadodiamide, PVP K90 polyvinylpyrrolidone K90, HP- $\beta$ -CyD hydroxypropyl-beta-cyclodextrin and ES-100 Eudragit S100.

subjected to ultra-sonication (Sonix SS 101H230, USA) for 5 min to get rid of any formed air bubbles.

## Preparation of Core NFs Solution

Three mL GDD was dissolved in 7 mL absolute ethanol to produce the core solution. An accurately weighed quantity of PVP (0.8 gm), HP- $\beta$ -CyD (1.85 gm), sodium saccharine (100 mg) and glycerol (0.2 mL) were added to GDD solution as shown in Table 2.<sup>22</sup> The volume was completed with absolute ethanol to produce 10 mL core solution. Subsequently, the solution was vortexed using vortex mixer (VM-300P, USA) for 30 min then ultra-sonication (Sonix SS 101H230, USA) for 15 min to discard any formed air bubbles.

## Spinning of Coaxial NFs

Coaxial electrospinning was performed using electrospinning apparatus (Nanon-OIA, MECC CO., Ltd., JAPAN) on a setup comprising two syringe pumps and a high voltage power supply. A concentric spinneret was employed for the electrospinning process: the outer needle internal diameter (I.D.) is 14 gauge, and the inner needle I. D. is 21 gauge.<sup>22,23</sup> After many trials for optimization of the procedure, the applied voltage was fixed at 25 kV, the core fluid flow rate was 0.3 mL/h and the sheath fluid rate was 1 mL/h. NFs were collected on a collector plate covered with aluminium foil placed at 12 cm from the spinneret. All experiments were performed under ambient conditions ( $25 \pm 2$  °C;  $57 \pm 6\%$  relative humidity).

GDD coaxial NFs were kept at  $-18$ °C for overnight, and freeze dried using freeze dryer (SIM FD8-8T, SIM international, USA) at  $-80$ °C under vacuum for 2 h then they were removed from the aluminium foil and stored in refrigerator at 4°C for further analysis.<sup>24</sup> Blank NFs, as a control, were prepared with the same composition without GDD loading.

## Characterization of GDD Loaded Coaxial NFs

### Scanning Electron Microscopy (SEM)

Scanning of coaxial NFs was done using electron microscopy (JSM-6150, JEOL, TOKYO, JAPAN) operated at an accelerating voltage of 20 kV to examine the morphology of NFs. Thin piece of NFS sheared from the center, using a sharp razor blade, and fixed on aluminum stubs with conductive double sided adhesive tape and coated with gold by sputter coater at 50 mA for 50 S. The average diameters of the individual NFs were measured using Image J Analysis Software (NIH, USA).<sup>25</sup>

### Differential Scanning Calorimetry (DSC)

Differential scanning calorimetry thermograms of lyophilized GDD powder, HP- $\beta$ -CyD, PVP K90, ES 100 each alone, their corresponding physical mixture and lyophilized coaxial NFs were analyzed by DSC (Perkin-Elmer 4, USA) using 5 mg sample of each component. Samples were spread and hermetically sealed in aluminum pans and heated at a constant rate of 5°C/min over a temperature range of 25°C–400°C. Inert atmosphere was maintained by purging nitrogen as a blank gas at a flow rate of 10°C/min.

### Attenuated Total Reflectance-Fourier Transform Infrared Spectroscopy (ATR-FTIR)

FTIR is a commonly used analytical tool for studying the chemical structure of sample. While attenuated total reflection (ATR) (Mattson 500 Madison Instruments, USA) is a sampling technique that simplifies sample preparation. Its mechanism of action based on entering the IR beam into the ATR crystal and is totally internally reflected at the interface between the crystal and the sample.<sup>26</sup> The reflection induces an evanescent field that penetrates the sample due to the wave-like properties. The penetration depth of the evanescent wave is typically in the order of a few microns (0.5–3  $\mu$ m) depending on the wavelength, the angle that IR beam enters the crystal, and the refractive indices of the ATR crystal and the sample.<sup>27</sup> The lyophilized GDD powder, HP- $\beta$ -CyD, PVP K90, ES-100 each alone, their corresponding physical mixture and the lyophilized coaxial NFs were placed on the top of ATR crystals and pressed with a stylus to insure intimate contact with it. The spectral range utilized extended from 400 to 4000  $\text{cm}^{-1}$  and the measurements were made by averaging 64 scans at a resolution of 4  $\text{cm}^{-1}$ . The observed absorption peaks were compared with known compounds to make assignments.<sup>28</sup>

### Thermogravimetric Analysis

The thermal stability of different samples was evaluated by TGA (Q500, TA Instruments, USA). TGA measure changes in the weight of samples as a function of temperature by heating samples from room temperature to 600 °C at constant heating rate of 10 °C  $\text{min}^{-1}$  under nitrogen atmosphere.

### Measurement of Hydration Capacity

Coaxial NFs pieces (25 mg) were added to 10 cm petri dish, containing 10 mL HCl (pH 1.2) simulating stomach pH. Then, the petri dish was kept at 37°C using a hot air oven (Gering model SPA-GELMAN Instrument No. 16,414, Germany). The swelling behavior was observed at predetermined time intervals; 15, 30, 45, 60, 75, 90, 105, 120 min and 24 h. At each time, samples were removed carefully from the petri dish and blotted off cautiously on tissue papers to remove the surface-adhered liquid droplets and reweighed to constant weight.<sup>29</sup> The experiment was done in triplicate and the mean values were calculated. The water uptake percent was calculated according to the following equation:

$$\text{Water uptake(\%)} = \frac{W_2 - W_1}{W_1} \times 100$$

where,

W2 is the weight of the hydrated NFs and W1 is the initial weight of NFs.

### Determination of Entrapment Efficiency (EE%)

Twenty-five mg of the freeze dried coaxial NFs were cutted and dissolved in 10 mL PB (pH 7.4) using a magnetic stirrer (Heidolph, USA) for 5 min until complete dissolution of the NFs. The drug content was analyzed spectrophotometrically using UV/VIS spectrophotometer (Jasco, Japan) at 202 nm after filtration and suitable dilution of the sample. The experiment was done in triplicate and the mean values were calculated. The entrapment efficiency percent (EE%) was calculated according to the following equation.<sup>30</sup>

$$\text{EE\%} = \frac{\text{Weight of drug in NFs}}{\text{Theoretical weight of drug in NFs}} \times 100$$

### In vitro Release Study

In vitro studies of the prepared GDD coaxial NFs (0.25 mg) were carried out in dissolution test apparatus USP II rotating basket (Abbott 8 cell Dissolution II

Apparatus, USA) in two different media at pH 1.2 using 500 mL 0.1N HCl for 2 h and 250 mL BP (pH 7.4) for 1 h. The temperature was adjusted at  $37 \pm 0.5^\circ\text{C}$  at the stirring rate; 100 rpm and 50 rpm, respectively.

Five milliliter of the dissolution media were taken at regular time interval of 2, 5, 10, 15, 30, 60, 90, 120 min for 0.1 N HCl and 2, 4, 6, 8, 10, 15, 30, 60 min for PB (pH 7.4). An equal volume of the respective dissolution medium was added to maintain the sink conditions throughout the experiment. The collected aliquots were filtered and further analyzed spectrophotometrically using UV/VIS spectrophotometer at 202 nm. A blank coaxial NFs were used to eradicate any possible interference. All measurements were done in triplicate from three independent samples and the mean values were calculated.

## Kinetic Analysis of Drug Release Data

The data of in vitro contrast agent release from the prepared coaxial NFs were analyzed mathematically using the following models zero-order and first-order and Higuchi's model.<sup>31,32</sup> The model with the highest correlation coefficient ( $r^2$ ) is the predominant one.<sup>33</sup>

## In vitro Cytotoxicity Study

### Cell Culture

To investigate the potential biological application of the coaxial GDD NFs, in vitro cytotoxicity study was done for GDD, the plain and medicated coaxial NFs using methyl thiazolyl tetrazolium (MTT) assay. A Human colorectal adenocarcinoma (Caco-2) was obtained from the American Type Culture Collection (Manassas, VA, USA). Caco-2 cells were cultured in complete cell culture medium (DMEM+) composed of: Dulbecco Modified Eagle's Minimal Essential medium (DMEM; 4.5 g/L glucose) supplemented with L-glutamine (Lonza, Belgium), non-essential amino acids (NEAA; 1% v/v; BioWhittaker, Lonza), penicillin-streptomycin (PEST; 1% v/v; Sigma, MO, USA), and heat-inactivated fetal bovine serum (FBS; 10% v/v; Gibco, MA, USA). Culture medium was refreshed every two day (at 80–85% confluence) using 0.25% trypsin and 0.02% ethylenediaminetetraacetic acid (EDTA).

### Cell Viability

Cell viability experiments ( $n=3$ ) were analyzed. Approximately 10,000 cells/well were seeded in 96-well plates 48h prior to exposure. The used concentrations were selected based on a previous study that showed absence of toxicity of 100, 200, 300 and 400  $\mu\text{g/mL}$  prepared GDD

nanoparticles to HeLa cells.<sup>34</sup> The plates were incubated for 24h at  $37^\circ\text{C}$  in an atmosphere of 5%  $\text{CO}_2$  and 90% relative humidity. The cells were then incubated in media with 0.1 mg/mL of tetrazolium (MTT dye) for 3 hours. The precipitated formazan was solubilized with 100  $\mu\text{L}$  dimethyl sulfoxide (DMSO). Culture medium without NFs or the drug was used as the control. Absorbance was measured at a wavelength of 450 nm using an ELX800 absorbance microplate reader (Bio-Tek Instruments, Inc., Winooski, VT, USA). Cytotoxicity was measured by measuring cell viability relative to that of control group cells using the following equation:<sup>35</sup>

$$\% \text{ Cell viability} = \frac{\text{OD treated}}{\text{OD plainmedia}} \times 100$$

where OD, The optical density.

### In vitro Evaluation Using X-Ray

X-ray evaluation was carried on; concentrated coaxial NFs solution (50 mg of freeze dried GDD coaxial NFs dissolved in 5 mL PB (pH 7.4)), diluted coaxial NFs solution (50 mg of freeze dried GDD-NFs dissolved in 15 mL PB (pH 7.4)), GDD solution (Omniscan) and water by loading these solutions inside syringes and positioned in mammography unit (Alpha ST Optimized Mammography, General Electric (G. E)).<sup>36</sup> Coaxial NFs containing GDD were evaluated using low-dose x-rays radiography (mammography) compared to commercial GDD and water at 33 kV and 120 mA.

## Result and Discussion

### Preparation of Coaxial NFs

PVP K90 is the main polymer used to prepare the core of the NFs containing GDD as it is known for its high water solubility so offers the onset release of GDD inside the colon which is essential for MRI contrast agent action.<sup>37</sup> HP- $\beta$ -CyD has a crucial role in the core formation as it is responsible for decreasing the hygroscopicity of PVP K90 and formation of a good spinned NFS.<sup>23,38</sup>

ES-100 is characterized by its low solubility in pH less than 7.4 so it protects the NFs from the acidic stomach.<sup>39</sup> Applied voltage, suitable needle internal diameter and falling distance were investigated and optimized. This coaxial NFs are likely to release GDD in the intestine for imaging.

### Characterization of the Prepared Coaxial NFs

#### Scanning Electron Microscopy (SEM)

SEM images of GDD coaxial NFs and GDD core NFS are illustrated in [Figure 1A](#) and [B](#) respectively. Electron

microscopy showed all the NFs to have cylindrical shapes. These images reveal that NFs have uniform structures without any “beads-on-a-string” morphology visible. Also, there is no evidence for any particles or phase separation present, indicating that the multiple components of the formulations are homogeneously mixed. It can be seen that all coaxial NFs are around  $2000 \pm 186$  nm in size, while the core fibers only are around  $361 \text{ nm} \pm 41$  nm. This result agreed with Illangakoon et al, 2015 who illustrated that coaxial NFs of 5-fluorouracil using ES 100 as shell can exceed 1000 nm.<sup>39</sup>

### Differential Scanning Calorimetry (DSC)

DSC examinations were conducted to study the thermal behavior of the lyophilized GDD NFs and the physical mixture of the components, Figure 2. The thermogram of the lyophilized GDD (Figure 2A) exhibited only one endothermic peak at  $86.3^\circ\text{C}$  which is attributed to transformation of GDD from crystal form to amorphous form.<sup>40</sup> The thermogram of HP- $\beta$ -CyD indicates a broad endothermic peak around  $70.9^\circ\text{C}$  which is attributed to the release of water of crystallization (Figure 2B).<sup>41</sup> The DSC thermogram of PVP K90 (Figure 2C) display an endothermic peak ranging from  $21^\circ\text{C}$  to  $103^\circ\text{C}$ , due to the loss of water from the hygroscopic PVP K90.<sup>42</sup>

For ES 100, there are two endothermic peaks, first one between  $30^\circ\text{C}$  and  $75^\circ\text{C}$  due to dehydration and a second one ranging from  $202^\circ\text{C}$  to  $230^\circ\text{C}$ , which may be due to thermal degradation (Figure 2D). These findings are consistent with other results documented by Illangakoon et al (2014) and Reda et al (2017).<sup>43,44</sup> The thermogram of the physical mixture (Figure 2E) reveals the corresponding melting endothermic peak of ES 100 with lower intensity, which may be due to the dilution effect.<sup>42</sup> However, that of

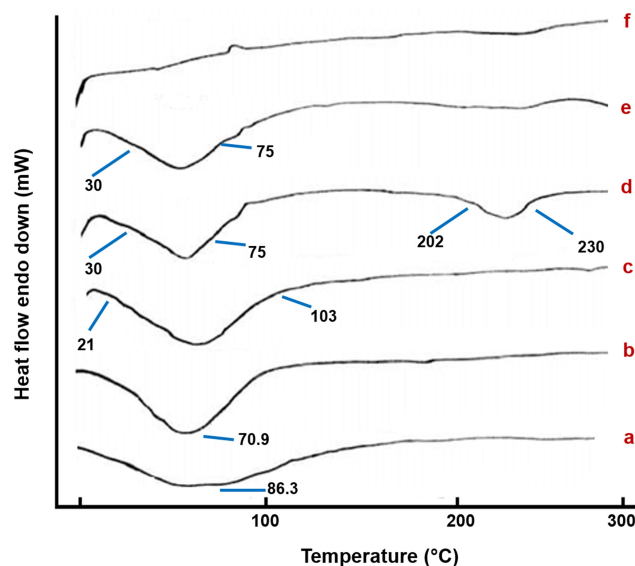


**Figure 2** DSC thermograms of lyophilized GDD (a), HP- $\beta$ -CyD (b), PVP K90 (c), ES 100 (d), physical mixture of NFs components (e) and coaxial NFs (f).

**Abbreviations:** DSC, differential scanning calorimetry; ES 100, Eudragit S100; GDD, gadodiamide; HP- $\beta$ -CyD, hydroxypropyl-beta-cyclodextrin; NFs, nanofibers; PVP K90, polyvinylpyrrolidone K90.

coaxial NFs (Figure 2F), no peaks were detected, suggesting an amorphous composite of GDD were formed. This may be attributed to the extremely rapid evaporation of the solvent from the fibers during the electrospinning process, resulting in the inability of the drug molecules to form crystalline aggregates or lattice within the NFs.<sup>45</sup>

### Attenuated Total Reflectance-Fourier Transform Infrared Spectroscopy (ATR-FTIR)

The ATR-FTIR spectra for the lyophilized GDD, HP- $\beta$ -CyD, PVP K90, ES 100, physical mixture, coaxial NFs mat are

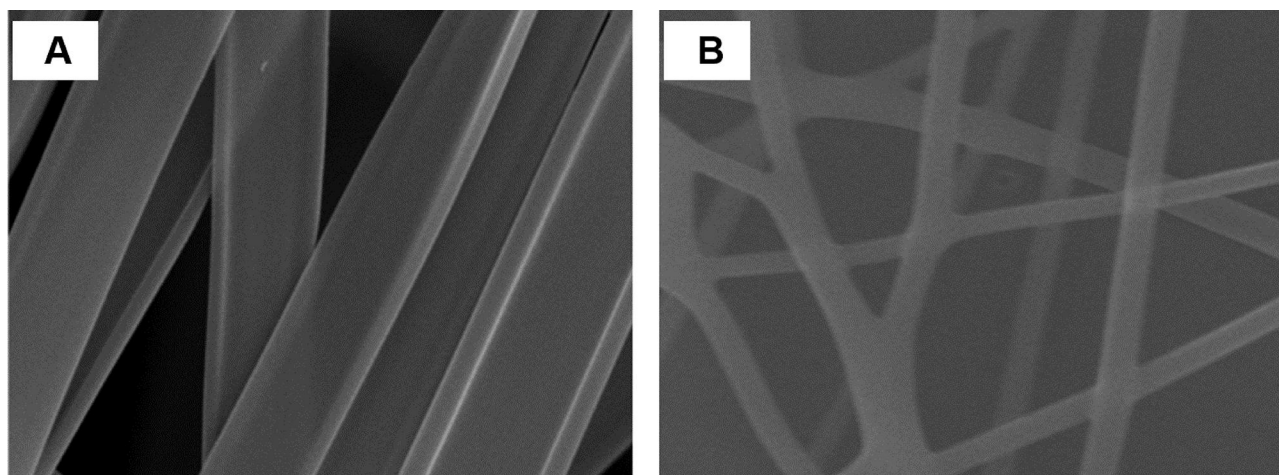


**Figure 1** SEM image of (A) GDD coaxial NFs and (B) GDD loaded core NFs.

**Abbreviations:** GDD, gadodiamide; NFs, nanofibers; SEM, scanning electron microscopy.

shown in Figure 3. Two well-defined, sharp peaks were visible for lyophilized GDD, one at  $700\text{ cm}^{-1}$  indicating the presence of GDD and another one at  $1582\text{ cm}^{-1}$  due to the stretching of the ketone group (Figure 3A). Besides, a dual peak around  $3500\text{ cm}^{-1}$  indicating the presence of amide and hydroxyl bonds.<sup>46</sup> In Figure 3B, the FT-IR spectrum of pure HP- $\beta$ -CyD is characterized by prominent peaks at  $3402\text{ cm}^{-1}$  for O-H,  $2954\text{ cm}^{-1}$  for C-H and  $1644\text{ cm}^{-1}$  for H-O-H bending.<sup>47</sup> The spectrum of the pure PVP K90 as in Figure 3C shows broad bands at  $3355\text{ cm}^{-1}$  for O-H stretches from residual water and  $2928\text{ cm}^{-1}$  for C-H stretching, as well as at  $1032\text{ cm}^{-1}$  that corresponds to the stretching vibrations of C-O. These data agree with those reported previously.<sup>38</sup>

FT-IR spectrum of pure ES 100, Figure 3D, displays characteristic bands of methyl and methylene C-H stretch vibrations at  $2949\text{ cm}^{-1}$  and a strong band of esterified carbonyl groups at  $1722\text{ cm}^{-1}$  (C=O stretch) and broad hydroxyl group absorption bands between  $3300$  and  $3600\text{ cm}^{-1}$ .<sup>44</sup> In both FT-IR spectra of GDD coaxial NFs and its physical mixture in Figure 3F and 3E, respectively, intense peaks from ES-100 are visible at  $1721\text{ cm}^{-1}$  (C=O stretch) and a second peak can be seen at  $1151\text{ cm}^{-1}$  due to C-O-C stretching. Additionally, the spectra show a strong peak at  $1643\text{ cm}^{-1}$  which may arise either from PVP K90 or from the HP- $\beta$ -CyD in the core.<sup>30</sup> Besides, the most

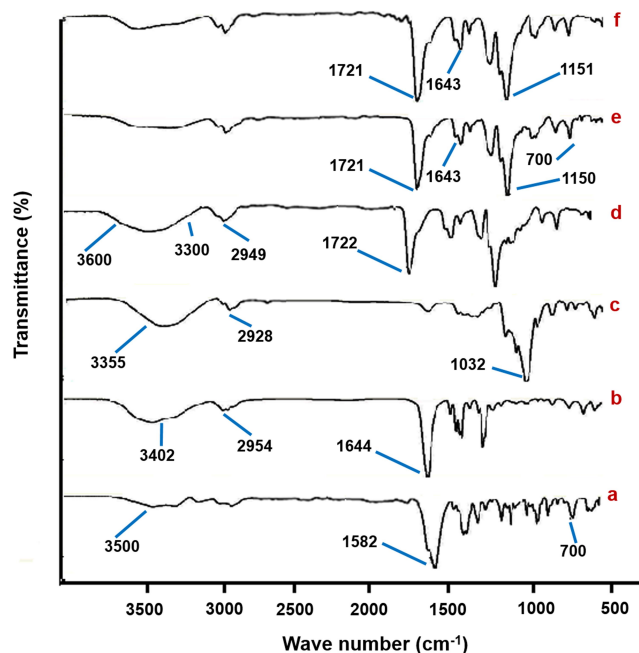


**Figure 3** ATR-FTIR spectra of lyophilized GDD (a), HP- $\beta$ -CyD (b), PVP K90 (c), ES 100 (d), physical mixture of NFs components (e) and coaxial NFs (f).

**Abbreviations:** ATR-FTIR, attenuated total reflectance-Fourier transform infrared spectroscopy; ES 100, Eudragit S100; GDD, gadodiamide; HP- $\beta$ -CyD, hydroxypropyl-beta-cyclodextrin; NFs, nanofibers; PVP K90, polyvinylpyrrolidone K90.

characteristic peak of GDD at  $700\text{ cm}^{-1}$  decreased extensively in the physical mixture and disappeared in NFs.

### Thermogravimetric Analysis

Thermal analysis is a predictable method for drugs quality control of pharmaceutical interest that provides useful information about the physical properties of materials.<sup>48</sup> Differential scanning calorimetry (DSC) and thermogravimetric analysis (TGA), either separately or together, are often the first step(s) in a comprehensive search for a property of a particular drug and for the determination of its compatibility, stability, and kinetic analysis.<sup>49</sup> Thermogravimetric methods have been used to determine drug stability either as non-isothermal TG (the temperature is elevated at a constant rate) or as isothermal TG (the temperature is set at a predetermined temperature).

The results of TGA and their respective derivative thermogravimetric analysis (DTG) of PVP K90, HP- $\beta$ -CyD, ES -100, GDD and coaxial NFs from  $25^{\circ}\text{C}$  to  $600^{\circ}\text{C}$  are shown in Figure 4. The maximum percentage mass change is

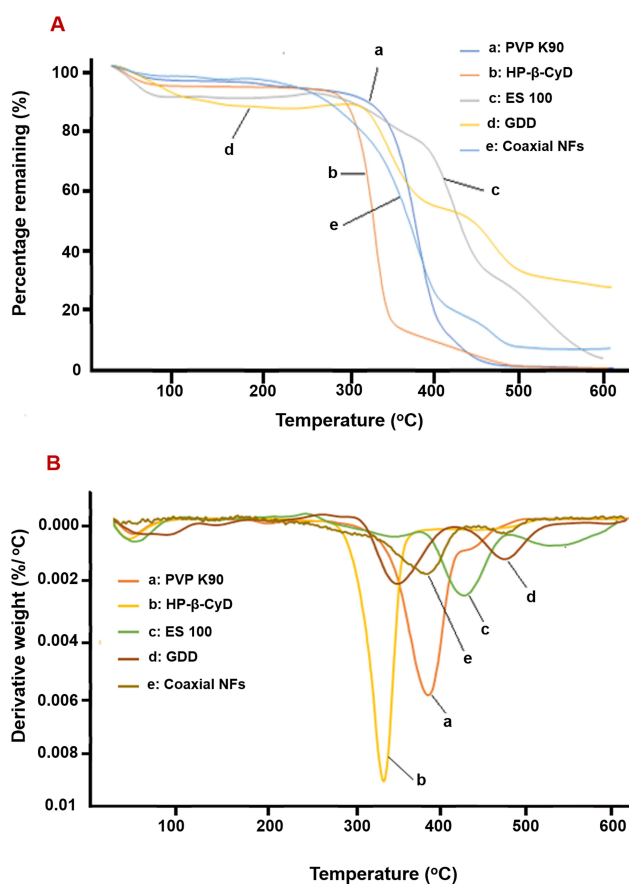


**Figure 4** TGA (A) and DTG (B) of different samples.

**Abbreviations:** TGA, thermogravimetric analysis; DTG, differential thermogravimetry.

experienced by NFs at 379.4°C followed by PVP K90 at 377°C (Figure 4).<sup>50</sup> All other ingredients including lyophilized GDD, HP-β-CyD and ES-100 show earlier change around 300 °C.<sup>51–54</sup> These results indicated that coaxial NFs effectively enhanced the thermal stability of encapsulated GDD.

### Measurement of Hydration Capacity

The rate and extent of coaxial NFs hydration and swelling may affect the mucoadhesion and, consequently, the drug release from the NFs.<sup>55</sup> The maximum hydration capacities of the samples were obtained within 15 min in 0.1 N HCl. The dry coaxial NFs could absorb large quantity of water about  $10.36 \pm 1.19$  times of their original dry weight. In general, the ability of ES 100 polymer to absorb water is due to the presence of water-soluble groups such as –COOH that formed hydrogen bond with the aqueous medium. Thus, the hydration of this group resulted in water entry into the polymer chain.<sup>56</sup> ES 100 is not completely hydrophilic, so, the less hydrophilic moiety of ES-100 resulted in the resistance of the matrix network structure, mainly hydrogen bonds, to the movement of water molecules. Thus, coaxial NFs did not show any appreciable changes in its shape and maintained the integrity of the NFs during the study period.

### Determination of Entrapment Efficiency (EE%)

The entrapment efficiency is regarded as a fundamental criteria for evaluation of the quantity of GDD in NFs. The EE% of GDD in NFs was  $94.3 \pm 3.1\%$  (w/w). This result agrees with Lin et al, 2020 as they proved that NFs made from PVP and HP-β-CyD have EE% more than 90%.<sup>57</sup> High entrapment efficacy % was expected because of the remarkable high surface area of the coaxial NFs and also as a result of the incorporation of the drug into the polymeric solution to be spun and solidify during the electrospinning process.<sup>58</sup> The drug was entrapped in the polymer fiber mat; therefore, the risk of drug loss during this process was low.

### In vitro Release Study

Figure 5 depicts the dissolution profile of GDD from the prepared coaxial NFs at pH 1.2 and 7.4 representing the stomach, and the small and large intestine, respectively. ES-100 is insoluble in pH less than 7, it is noticed that a burst release of about  $11.74 \pm 2.02\%$  of the GDD occurred in the first 2 min and did not exceed  $13.25 \pm 3.95\%$  of GDD through the 2 h. These observations might be due to GDD escape from the ES-100 coat. In addition, some fibers were observed to be broken or merged through 2 h at pH 1.2, providing additional escape routes for the

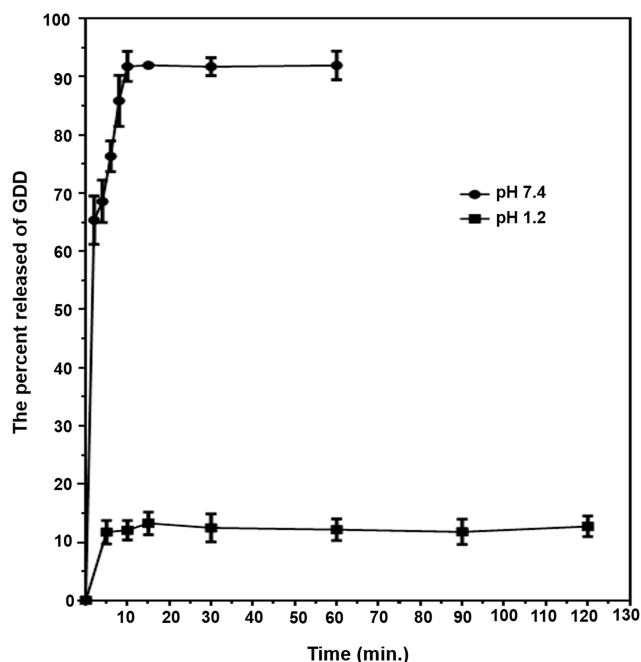


**Figure 5** In vitro release of GDD from the prepared coaxial NFs in pH 1.2 for 2 h and in pH 7.4 for 1 h.

**Note:** Each point represents the mean  $\pm$  SD (n=3).

**Abbreviations:** GDD, gadodiamide; NFs, nanofibers.

GDD. Meanwhile, in pH 7.4, the sheath of coaxial NFs was completely disintegrated within few min, leaving the core of the NFs to release GDD. Hence, the drug release reached to  $91.76\% \pm 2.58\%$  after 10 min.

From the obtained result it is obvious that: firstly, the formulation of coaxial NFs successfully retained GDD from being released in the gastric pH for 2 h.<sup>39</sup> Secondly, in the small and large intestine pH, NFs swiftly disintegrated due to the solubility of ES 100 in the basic medium with the release of GDD.<sup>44</sup> It was noticeable that the fiber mat had virtually completely disintegrated (degrade) within few seconds in pH 7.4. Conversely in pH 1.2, the shape of fiber has not changed. Finally, the results obviously depict that a remarkable increase in % GDD release was detected in PB (pH 7.4). This indicates more extent of GDD release at the site of action (small and large intestine) with subsequent, increase in contrast agent efficacy. This result is consistent with Ding et al, they reported that ES-100 shell had a better performance to prevent drug release in the stomach.<sup>59</sup>

### Kinetic Analysis of the Release Data

The kinetic analysis of the release data (Table 3) was reliant on the medium pH. In both media, the release data were best fitted with Higushi's model.



**Table 3** Kinetic Analysis of the Percentage Drug Released

Dissolution Medium	Coefficient of Determination ( $r^2$ )		
	Zero-Order	First-Order	Higuchi Model
0.1N HCl (pH 1.2)	0.653	0.624	0.851
Phosphate buffer (pH 7.4)	0.716	0.903	0.918

**Notes:**  $r^2$  is the coefficients of determination; and  $n$  is diffusional exponent. Dissolution medium of coaxial NFs in 0.1N HCl (pH 1.2) for 2 h and in phosphate buffer (pH 7.4) for 1 h.

### In vitro Cytotoxicity Study

Figure 6 demonstrates that there is insignificant cytotoxicity after 24 h of incubation with GDD ( $P > 0.05$ ), the plain and medicated coaxial NFs within the detected concentration range. Even at the highest concentration of 400  $\mu\text{g/mL}$  of the medicated coaxial NFs, the viabilities of Caco-2 cells still maintained  $82.5\% \pm 1.2$ . This result is in agreement with the results of other studies.<sup>34,60</sup>

Previous studies demonstrated in vitro cytotoxicity of  $\text{Gd}^{3+}$  using different cell line. Perera et al studied the in vitro cytotoxicity of Gd-NPs using the HT-29 cells. The results clearly indicated that the NPs are nontoxic to cells.<sup>60</sup> Also, the cytotoxicity of PEG-coated and Gd-loaded fluorescent silica NPs using LNCaP and PC3 Cells was studied by Jiang et al. They found no significant

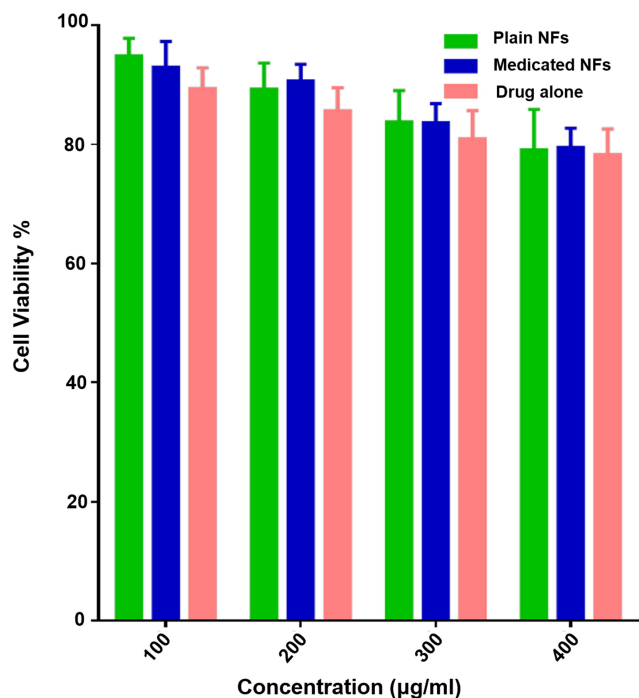


**Figure 6** Cytotoxicity against Caco-2 cells after incubation with GDD, the plain and medicated coaxial NFs for 24 h.

**Note:** Results represent the mean  $\pm$  SEM ( $n=3$ ). **Abbreviations:** GDD, gadodiamide; NFs, nanofibers.

cytotoxicity after 24 h of incubation with NPs, suggesting that these NPs exhibited no toxicity toward LNCaP and PC3 cells.<sup>61</sup>

Nörenberg et al examined the potential gadolinium (Gd) accumulation in the brain of healthy mice after long-term oral administration of Gd-containing food pellets and investigated whether Gd could lead to adverse central nervous system (CNS) effects. They suggested that low levels of intracerebral Gd do not lead to detectable CNS effects, and in particular did not impair locomotor abilities in the healthy murine model, even over a very long exposure time.<sup>62</sup>

### In vitro Evaluation Using X-Ray

Radiopacity has been done to test the absence of the coating material in the coaxial nanofibers on the response of GDD to X-ray. A simple estimate of radiopacity can be gained by subjecting the coaxial NFs to a standard X-ray. In the mammography, both coaxial NFs (concentrated (10 mg/mL) and diluted (3.33 mg/mL)) resulted in bright images (Figure 7). The attenuation of the signal intensity was much larger when the coaxial NFs concentration increased. For comparison, the GDD solution (287mg/mL) gives the whiter image. Fortunately, the coaxial NFs (with bright image) succeeded in the radiopacity test. This result encourages its use as MRI contrast agent.

### Conclusion

An oral dosage form for GDD was successfully maneuvered through electrospinning. Thermal analysis and in vitro cytotoxicity were manipulated to insure the stability and the safety of the prepared NFs. X-ray mammography of the NFs confirmed its ability to replace plain GDD as

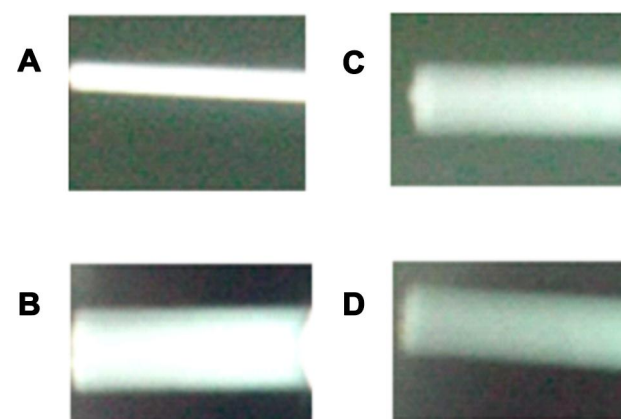


**Figure 7** In vitro evaluation using X-ray of GDD solution (A), concentrated solution of coaxial NFs (10 mg/mL) (B), diluted solution of coaxial NFs (3.33 mg/mL) (C), and water (D).

a contrast agent. The coaxial NFs loaded with GDD is a promising oral pharmaceutical dosage form for small and large intestine MRI, probably with reduced side effects. It might be speculated that this coaxial dosage form design could be applied for peptide oral absorption as well as theranostic. Further research work should be addressed.

## Disclosure

The authors report no conflicts of interest for this work.

## References

- Caster JM, Patel AN, Zhang T, Wang A. Investigational nanomedicines in 2016: a review of nanotherapeutics currently undergoing clinical trials. *Wiley Interdiscip Rev Nanomed Nanobiotechnol*. 2017;9(1):e1416. doi:10.1002/wnan.1416
- Yang Y, Wang X, Liao G, et al. iRGD-decorated red shift emissive carbon nanodots for tumor targeting fluorescence imaging. *J Colloid Interface Sci*. 2018;509:515–521. doi:10.1016/j.jcis.2017.09.007
- Nagarajan S, Soussan L, Bechelany M, et al. Novel biocompatible electrospun gelatin fiber mats with antibiotic drug delivery properties. *J Mater Chem B*. 2016;4(6):1134–1141. doi:10.1039/C5TB01897H
- Nagarajan S, Belaid H, Pochat-Bohatier C, et al. Design of boron nitride/gelatin electrospun nanofibers for bone tissue engineering. *ACS Appl Mater Interfaces*. 2017;9(39):33695–33706. doi:10.1021/acsami.7b13199
- Yu DG, Yu JH, Chen L, Williams GR, Wang X. Modified coaxial electrospinning for the preparation of high-quality ketoprofen-loaded cellulose acetate nanofibers. *Carbohydr Polym*. 2012;90(2):1016–1023. doi:10.1016/j.carbpol.2012.06.036
- Yarin A. Coaxial electrospinning and emulsion electrospinning of core-shell fibers. *Polym Adv Technol*. 2011;22(3):310–317. doi:10.1002/pat.1781
- Han T, Yarin AL, Reneker DH. Viscoelastic electrospun jets: initial stresses and elongational rheometry. *Polymer*. 2008;49(6):1651–1658. doi:10.1016/j.polymer.2008.01.035
- Alghoraibi I, Alomari S. Different methods for nanofiber design and fabrication. *Handbook Nanofibers*. 2018;1–46. doi:10.1007/978-3-319-42789-8\_11-2
- Busato A, Feruglio PF, Parnigotto P, et al. In vivo imaging techniques: a new era for histochemical analysis. *Eur J Histochem*. 2016;60(4):2725. doi:10.4081/ejh.2016.2725
- Siegrist M. Predicting the future: review of public perception studies of nanotechnology. *Hum Ecol Risk Assess*. 2010;16(4):837–846. doi:10.1080/10807039.2010.501255
- Na HB, Hyeon T. Nanostructured T1 MRI contrast agents. *J Mater Chem*. 2009;19(35):6267–6273. doi:10.1039/B902685A
- Na HB, Song IC, Hyeon T. Inorganic nanoparticles for MRI contrast agents. *Adv Mater*. 2009;21(21):2133–2148. doi:10.1002/adma.200802366
- TF M, Gambhir SS. Molecular imaging in living subjects: seeing fundamental biological processes in a new light. *Genes Dev*. 2003;17(5):545–580. doi:10.1101/gad.1047403
- Si R, Zhang Y-W, Zhou H-P, et al. Controlled-synthesis, self-assembly behavior, and surface-dependent optical properties of high-quality rare-earth oxide nanocrystals. *Chem Mater*. 2007;19(1):18–27. doi:10.1021/cm0618392
- Zhao F, Yuan M, Zhang W, Gao S. Monodisperse lanthanide oxysulfide nanocrystals. *J Am Chem Soc*. 2006;128(36):11758–11759. doi:10.1021/ja0638410
- Vidaud C, Bourgeois D, Meyer D. Bone as target organ for metals: the case of f-elements. *Chem Res Toxicol*. 2012;25(6):1161–1175. doi:10.1021/tx300064m
- Feng X, Xia Q, Yuan L, Yang X, Wang K. Impaired mitochondrial function and oxidative stress in rat cortical neurons: implications for gadolinium-induced neurotoxicity. *Neurotoxicology*. 2010;31(4):391–398. doi:10.1016/j.neuro.2010.04.003
- Sherry AD, Caravan P, Lenkinski RE. Primer on gadolinium chemistry. *J Magn Reson Imaging*. 2009;30(6):1240–1248. doi:10.1002/jmri.21966
- Schneider G, Reimer P, Mamann A, Kirchin MA, Morana G, Grazioli L. Contrast agents in abdominal imaging: current and future directions. *Top Magn Reson Imaging*. 2005;16(1):107–124. doi:10.1097/01.rmr.0000189025.80743.5c
- Frisch A, Walter TC, Hamm B, Denecke T. Efficacy of oral contrast agents for upper gastrointestinal signal suppression in MRCP: a systematic review of the literature. *Acta Radiol*. 2017;6(9):1–7. doi:10.1177/2058460117727315
- Naito S, Tazaki H, Okamoto T, et al. Comparison of nephrotoxicity between two gadolinium-contrasts, gadodiamide and gadopentetate in patients with mildly diminished renal failure. *J Toxicol Sci*. 2007;42(3):379–384. doi:10.2131/jts.42.379
- Maslakci NN, Ulusoy S, Uygun E, et al. Ibuprofen and acetylsalicylic acid loaded electrospun PVP-dextran nanofiber mats for biomedical applications. *Polym Bull (Berl)*. 2017;74(8):3283–3299. doi:10.1007/s00289-016-1897-7
- Costoya A, Concheiro A, Alvarez-Lorenzo C. Electrospun fibers of cyclodextrins and poly (cyclodextrins). *Molecule*. 2017;22(2):230. doi:10.3390/molecules22020230
- Nune M, Krishnan UM, Sethuraman S. Decoration of PLGA electrospun nanofibers with designer self-assembling peptides: a “Nano-on-Nano” concept. *RSC Adv*. 2015;5(108):88748–88757. doi:10.1039/C5RA13576A
- Zhou W, Wang ZL. *Scanning Microscopy for Nanotechnology: Techniques and Applications*. New York, USA: Springer science and business media, spring street; 2007.
- Hassan MI, Sultana N. Characterization, drug loading and antibacterial activity of nanohydroxyapatite/polycaprolactone (nHA/PCL) electrospun membrane. *3 Biotech*. 2017;7(4):249. doi:10.1007/s13205-017-0889-0
- Liu W Preparation and characterization of multi-layer biodegradable nanofibers by coaxial electrospinning and their potential for tissue engineering. PhD [dissertation]. University of Delaware. 2015.
- Yaman N, Velioglu SD. Use of Attenuated Total Reflectance—Fourier Transform Infrared (ATR-FTIR) Spectroscopy in combination with multivariate methods for the rapid determination of the adulteration of grape, Carob and Mulberry Pekmez. *Foods*. 2019;8(7):231. doi:10.3390/foods8070231
- Adua DC Jr, Hammer JA, Yuan Q, et al. Semi-interpenetrating network (sIPN) gelatin nanofiber scaffolds for oral mucosal drug delivery. *Acta Biomater*. 2013;9(5):6576–6584. doi:10.1016/j.actbio.2013.02.006
- Karthikeyan K, Guhathakarta S, Rajaram R, Korrapati PS. Electrospun zein/eudragit nanofibers based dual drug delivery system for the simultaneous delivery of aceclofenac and pantoprazole. *Int J Pharm*. 2012;438(1–2):117–122. doi:10.1016/j.ijpharm.2012.07.075
- Martin AN, Bustamante P, Chun AHC. *Physical Pharmacy: Physical Chemical Principles in the Pharmaceutical Sciences*. 4th ed. Philadelphia (Pa.): Lea & Febiger; 1993:284–323.
- Higuchi T. Mechanism of sustained-action medication. Theoretical analysis of rate of release of solid drugs dispersed in solid matrices. *J Pharm Sci*. 1963;52(12):1145–1149. doi:10.1002/jps.2600521210
- Tadros MI. Controlled-release effervescent floating matrix tablets of ciprofloxacin hydrochloride: development, optimization and in vitro-in vivo evaluation in healthy human volunteers. *Eur J Pharm Biopharm*. 2010;74(2):332–339. doi:10.1016/j.ejpb.2009.11.010
- Zhao L, Ge X, Yan G, et al. Double-mesoporous core-shell nanosystems based on platinum nanoparticles functionalized with lanthanide complexes for in vivo magnetic resonance imaging and photothermal therapy. *Nanoscale*. 2017;9(41):16012–16023. doi:10.1039/c7nr04983h

35. Benov L. Effect of growth media on the MTT colorimetric assay in bacteria. *PLoS One*. 2019;14(8):e0219713. doi:10.1371/journal.pone.0219713
36. Goodfriend AC, Welch TR, Nguyen KT, et al. Poly (gadodiamide fumaric acid): a bioresorbable, radiopaque, and MRI-visible polymer for biomedical applications. *ACS Biomater Sci Eng*. 2015;1(8):677–684. doi:10.1021/acsbomaterials.5b00091
37. Dai M, Jin S, Nugen SR. Water-soluble electrospun nanofibers as a method for on-chip reagent storage. *Biosensors*. 2012;2(4):388–395. doi:10.3390/bios2040388
38. Samprasit W, Akkaramongkolporn P, Kaomongkolgit R, Opanasopit P. Cyclodextrin-based oral dissolving films formulation of taste-masked meloxicam. *Pharm Dev Technol*. 2018;23(5):530–539. doi:10.1080/10837450.2017.1401636
39. Illangakoon UE, Yu D-G, Ahmad BS, et al. 5-Fluorouracil loaded Eudragit fibers prepared by electrospinning. *Int J Pharm*. 2015;495(2):895–902. doi:10.1016/j.ijpharm.2015.09.044
40. Skupin-Mrugalska P, Sobotta L, Warowicka A, et al. Theranostic liposomes as a bimodal carrier for magnetic resonance imaging contrast agent and photosensitizer. *J Inorg Biochem*. 2018;180:1–14. doi:10.1016/j.jinorgbio.2017.11.025
41. Suta L-M, Vlaia L, Fulas A, Ledeti I, Hadaruga D, Mircioiu C. Evaluation study of the inclusion complexes of some oximacs with 2-hydroxypropyl-β-cyclodextrin. *Rev Chim*. 2013;64(11):1279–1283.
42. Illangakoon UE, Nazir T, Williams GR, Chatterton NP. Mebeverine-loaded electrospun nanofibers: physicochemical characterization and dissolution studies. *J Pharm Sci*. 2014;103(1):283–292. doi:10.1002/jps.23759
43. Reda RI, Wen MM, El-Kamel AH. Ketoprofen-loaded Eudragit electrospun nanofibers for the treatment of oral mucositis. *Int J Nanomedicine*. 2017;12:2335–2351. doi:10.2147/IJN.S131253
44. Jahangiri A, Barzegar-Jalali M, Javadzadeh Y, et al. Physicochemical characterization of atorvastatin calcium/ezetimibe amorphous nano-solid dispersions prepared by electro-spraying method. *Artif Cells Nanomed Biotechnol*. 2017;45(6):1138–1145. doi:10.1080/21691401.2016.1202262
45. Tungprapa S, Jangchud I, Supaphol P. Release characteristics of four model drugs from drug-loaded electrospun cellulose acetate fiber mats. *Polymer*. 2007;48(17):5030–5041. doi:10.1016/j.polymer.2007.06.061
46. Oliveira AFD, Ferreira TH, Sousa EMBD, Lacerda MA. Silica nanoparticles containing 159-Gadolinium as potential system for cancer treatment. *INAC*. 2013.
47. George S, Vasudevan D. Studies on the preparation, characterization, and solubility of 2-HP-β-cyclodextrin-mecizline HCl inclusion complexes. *J Young Pharm*. 2012;4(4):220–227. doi:10.4103/0975-1483.104365
48. Cides LCS, Araújo AAS, Santos-Filho M, Matos JR. Thermal behavior, compatibility study and decomposition kinetics of glimepiride under isothermal and non-isothermal conditions. *J Therm Anal Calorim*. 2006;84(2):441–445. doi:10.1007/s10973-005-7131-8
49. Perpe'tuo GL, Gálico DA, Fugito RA, et al. Thermal behavior of some antihistamines. *J Therm Anal Calorim*. 2013;111(3):2019–2028. doi:10.1007/s10973-012-2247-0
50. Silva MF, Da Silva CA, Fogo FC, Pineda EAG, Hechenleitner AA. Thermal and FTIR study of polyvinylpyrrolidone/lignin blends. *J Therm Anal Calorim*. 2005;79(2):367–370. doi:10.1007/s10973-005-0066-2
51. Han D, Han Z, Liu L, et al. Solubility enhancement of myricetin by inclusion complexation with Heptakis-O-(2-Hydroxypropyl)-β-cyclodextrin: a joint experimental and theoretical study. *Int J Mol Sci*. 2020;21(3):766. doi:10.3390/ijms21030766
52. Vlachou M, Kikionis S, Siamidi A, et al. Development and characterization of Eudragit®-based electrospun nanofibrous mats and their formulation into nanofiber tablets for the modified release of furosemide. *Pharmaceutics*. 2019;11(9):480. doi:10.3390/pharmaceutics11090480
53. Dong X, Ding Y, Wu P, Wang C, Schäfer CG. Preparation of MRI-visible gadolinium methacrylate nanoparticles with low cytotoxicity and high magnetic relaxivity. *J Mater Sci*. 2017;52(13):7625–7636. doi:10.1007/s10853-017-1070-1
54. Sani Usman M, Hussein MZ, Fakurazi S, Masarudin MJ, Ahmad Saad FF. Gadolinium-doped gallic acid-zinc/aluminium-layered double hydroxide/gold theranostic nanoparticles for a bimodal magnetic resonance imaging and drug delivery system. *Nanomaterials*. 2017;7(9):244. doi:10.3390/nano7090244
55. Deore V, Kumar R, Gide P. Development and statistical optimization of mucoadhesive buccal patches of indomethacin, In Vitro and ex vivo evaluation. *Int J Adv Pharm Biol Chem*. 2013;2:405–422.
56. Auda SH, Ahmed MM, El-Rasoul SA, Saleh K. Formulation and physicochemical characterization of piroxicam containing polymer films. *Bull Pharm Sci*. 2010;33:33–42.
57. Lin YC, Hu SCS, Huang PH, Lin TC, Yen FL. Electrospun resveratrol-loaded polyvinylpyrrolidone/cyclodextrin nanofibers and their biomedical applications. *Pharmaceutics*. 2020;12(6):552. doi:10.3390/pharmaceutics12060552
58. Son YJ, Kim WJ, Yoo HS. Therapeutic applications of electrospun nanofibers for drug delivery systems. *Arch Pharm Res*. 2014;37(1):69–78. doi:10.1007/s12272-013-0284-2
59. Ding Y, Dou C, Chang S, et al. Core-shell eudragit s100 nanofibers prepared via triaxial electrospinning to provide a colon-targeted extended drug release. *Polymers*. 2020;12(9):2034. doi:10.3390/polym12092034
60. Perera VS, Chen G, Cai Q, Huang SD. Nanoparticles of gadolinium-incorporated Prussian blue with PEG coating as an effective oral MRI contrast agent for gastrointestinal tract imaging. *Analyst*. 2016;141(6):2016–2022. doi:10.1039/C5AN01873K
61. Jiang W, Fang H, Liu F, et al. PEG-coated and Gd-loaded fluorescent silica nanoparticles for targeted prostate cancer magnetic resonance imaging and fluorescence imaging. *Int J Nanomedicine*. 2019;14:5611–5622. doi:10.2147/IJN.S207098
62. Nörenberg D, Schmidt F, Schinke K, et al. Investigation of potential adverse central nervous system effects after long term oral administration of gadolinium in mice. *PLoS One*. 2020;15(4):e0231495. doi:10.1371/journal.pone.0231495

## International Journal of Nanomedicine

### Publish your work in this journal

The International Journal of Nanomedicine is an international, peer-reviewed journal focusing on the application of nanotechnology in diagnostics, therapeutics, and drug delivery systems throughout the biomedical field. This journal is indexed on PubMed Central, MedLine, CAS, SciSearch®, Current Contents®/Clinical Medicine,

Submit your manuscript here: <https://www.dovepress.com/international-journal-of-nanomedicine-journal>

Dovepress

Journal Citation Reports/Science Edition, EMBASE, Scopus and the Elsevier Bibliographic databases. The manuscript management system is completely online and includes a very quick and fair peer-review system, which is all easy to use. Visit <http://www.dovepress.com/testimonials.php> to read real quotes from published authors.